Nonisothermal and Isothermal Crystallization Kinetics of Nylon-12

Neil L. A. McFerran, Cecil G. Armstrong, Tony McNally

School of Mechanical and Aerospace Engineering, Queen's University Belfast, Belfast BT9 5AH, United Kingdom

Received 28 February 2008; accepted 11 May 2008
DOI 10.1002/app.28696
Published online 10 July 2008 in Wiley InterScience (www.interscience.wiley.com).

ABSTRACT: The isothermal and nonisothermal crystallization behavior of Nylon 12 was investigated using differential scanning calorimetry (DSC). An Avrami analysis was used to study the isothermal crystallization kinetics of Nylon 12, the Avrami exponent (n) determined and its relevance to crystal growth discussed and an activation energy for the process evaluated using an Arrhenius type expression. The Lauritzen and Hoffman analysis was used to examine the spherulitic growth process of the primary crystallization stage of Nylon 12. The surface-free energy and work of chain folding were calculated using a procedure reported by Hoffmann and the work of chain folding per molecular fold (σ) and chain stiffness of Nylon 12 (q) was calculated and compared to values reported for Nylons 6,6 and 11. The Jeziorny modification of the Avrami analysis, Cazé and Chuah average Avrami parameter methods and Ozawa equation were used in an attempt to model the nonisothermal crystallization kinetics of Nylon 12. A combined Avrami and Ozawa treatment, described by Liu, was used to more accurately model the nonisothermal crystallization kinetics of Nylon 12. The activation energy for nonisothermal crystallization processes was determined using the Kissinger method for Nylon 12 and compared with values reported previously for Nylon 6,6 and Nylon 11. © 2008 Wiley Periodicals, Inc. J Appl Polym Sci 110: 1043–1058, 2008

Key words: nylon 12; isothermal crystallization kinetics; nonisothermal crystallization kinetics; DSC

INTRODUCTION

The properties of semicrystalline polymers are determined not only by their chemical structure, chain conformation, and molecular weight distribution but also by the mechanisms and kinetics of crystallization. In conventional melt processing of polymers, crystallization behavior and kinetics are controlled by the thermal and shear history the polymer is subjected to, which in turn determine the basic morphology of the polymer, including the ratio of crystalline to amorphous phase, crystallite size, and geometry and the extent of the interfacial region between crystalline and amorphous phases. Crystallization from the melt proceeds at a finite rate under nonequilibrium conditions following a process of nucleation, crystal growth until a pseudoequilibrium of crystallinity is achieved.[1] Evans[2] likened the nucleation and crystallization process to the effect of raindrops falling into a pool first described by Poisson,[3] in that, each raindrop falls randomly on a surface of water creating one leading expanding circular wave, thus the probability, $P_n(t)$ that n waves will pass over a representative point, X up to a time t is exactly n. The solution is given by the Poisson distribution:

$$P_n(t) = e^{-E}(E^n/n!) \tag{1}$$

where E is the expected number of waves available by evaluation of the average number of counts of a large number of samples or by computation. To treat Poisson's problem as an analog for crystallization one may assume a thin layer of melt crystallizes by the formation of two-dimensional spherulties.[3] The probability that a randomly chosen point is not reached by any of the circularly spreading crystal aggregates ($n = 0$), i.e., the point remains amorphous is given by:

$$P_o(t) = e^{-E} = 1 - v^c \tag{2}$$

where v^c is the volume fraction of the material crystallized. Equation (2) is the basis for the general form of the Avrami equation, modified by Evans[2] and first used by Mears[4] and Hay[5] to describe the crystallization kinetics of semicrystalline polymers. The crystallization behavior[6,7] and kinetics of polymeric materials has been reviewed previously.[8–10] In particular, the isothermal and nonisothermal crystallization kinetics of isotactic polypropylene,[11–13] filled polypropylenes,[14,15] polypropylene blends,[16–18] poly (ethylene terephthalate)[19,20] (PET) and PET

Correspondence to: T. McNally (t.mcnally@qub.ac.uk).

copolymers[21–23] have been investigated in detail, and to a much lesser extent engineering polymers such as poly(sulfides)[24–26] and poly(ketones).[27,28] Many nylon, including homopolymers, copolymers and filled systems have also been studied, but most of the crystallization kinetic studies have been limited to nylons 6,[29–31] 6,6,[32,33] 11,[34] and 12,12.[35,36] In this article, we report and test the validity of a range of mathematical models to describe the isothermal and nonisothermal crystallization kinetics of Nylon 12, hitherto not investigated in detail for Nylon 12, an important engineering plastic that finds widespread application in the automotive and consumer industries.

EXPERIMENTAL

The Nylon 12 used in this study was a Vestamid LX9002 black 9.7507, provided by Degussa high performance polymers, Germany. This grade of Nylon 12 is a plasticized compound with heat and light stabilizer and 13% carbon black coloring. It is used commercially in automotive multilayer tubing. The material has a Melt Volume Ratio (MVR) of 10 cm^3/10 min (ISO1133), $M_w = 172800$ and a $M_n = 14400$. The samples were dried in a convection oven at 348 K for 48 h before use to remove any residual moisture within the samples.

The isothermal crystallization investigation was completed using a Perkin–Elmer diamond DSC controlled by Pyris software. This unit is a power compensated differential scanning calorimeter, the sample and reference material each confined to separate self-contained calorimeters. The temperature is measured using platinum resistance thermometers that utilize a unique thermal guard system, a combination of trapped air, high-tech epoxies and aluminized coatings that allows superior baseline reproducibility that permits more accurate heating and cooling rates, up to 500 K/min, vital for accurate measurements required for isothermal studies. For the isothermal investigation the samples were initially heated at 20 K/min from 303 to 493 K. The samples were held at 493 K for 10 min to eliminate any residual crystals within the Nylon 12 samples. The samples were then cooled at 300 K/min to a range of set crystallization temperatures, 435 K (162°C), 433 K (160°C), 429 K (156°C), 427 K (154°C), 425 K (152°C), 423 K (150°C), and 421 K (148°C). The samples were held at these temperatures for 15 min to promote isothermal crystallization then cooled to ambient at 150 K/min. The curves for heat flow as a function of time were recorded for each isothermal crystallization temperature.

Nonisothermal crystallization kinetics was studied using a Perkin–Elmer DSC-VI differential scanning calorimeter and tests performed under a nitrogen atmosphere. The nonisothermal crystallization and melting cycle was set to study the formation of crystallites in Nylon 12 dependent on different cooling rates. The samples were heated at 20 K/min to 493 K, 30 K above the melting temperature (T_m) of this Nylon 12, and held there for 10 min to eliminate residual crystals in the melt. The melt was then cooled at different cooling rates to ambient, 5, 10, 15, 20, 25, 30, 35, and 40 K/min. The exothermic curves of heat flow as a function of both time and temperature were recorded for each cooling rate. All samples (8.5–9 mg) were cut from dried extruded Nylon 12 cast film of 15 μm thickness to maximize thermal conduction between the sample and pan.

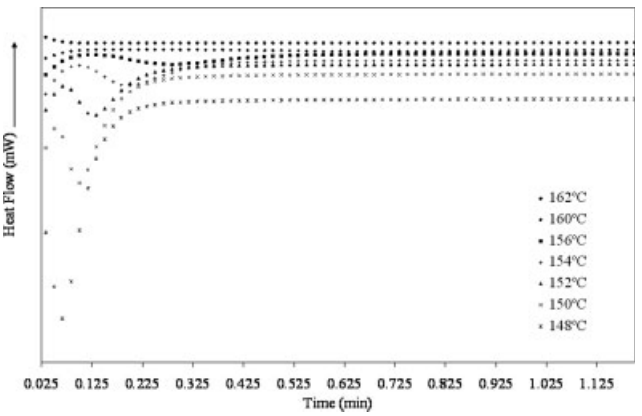

Figure 1 Heat flow versus time during isothermal crystallization of Nylon 12 at different crystallization temperatures cooled from 493 K.

RESULTS AND DISCUSSION

Isothermal crystallization

Isothermal crystallization kinetics and Avrami equation

The crystallization curves for each temperature are shown in Figure 1. It can be seen that as the crystallization temperature (T_c) was increased, the crystallization endotherms were shifted to longer time scales and became progressively less intense. This implies that the total crystallization time was extended and the crystallization rate decreased with increased crystallization temperature. The least squares method was used to integrate each of the crystallization curves at set intervals of time, between the onset and offset times. For comparative purposes the onset time was taken as zero for each isothermal crystallization study. A plot of $X(t)$, (relative crystallinity in terms of time) versus time (mins) was produced from this integration and shows the time taken for $X(t)$ to equal 1, see Figure 2. As T_c was increased, the time in which crystallization occurs became progressively longer and can be considered

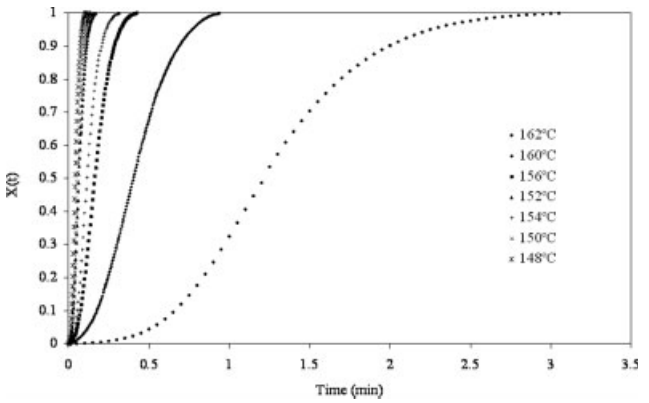

Figure 2 $X(t)$ versus time for isothermal crystallization process of Nylon 12.

in terms of the quenching the sample undergoes when cooled from the melt. At higher crystallization temperatures (circa. 162°C) the material was only 14 K below the T_m of Nylon 12, crystallization was therefore not driven by a large temperature gradient and occurred over a longer period of time as evident in Figures 1 and 2. As the temperature gradient between the melt and crystallization temperatures increased, the time at which the onset of crystallization occurs, the total time for crystallization and the shape of the crystallization endotherm changed markedly. As the crystallization temperature was decreased and the sample reached the desired temperature, the onset time of crystallization decreased accordingly, see Figure 1. The sample was effectively quenched when cooled, thus crystallization occurred rapidly over a much shorter time scale, again apparent from Figures 1 and 2. The crystallization endotherm also became much sharper as the crystallization temperature was increased due to the increased rate of crystallization, a consequence of the larger temperature gradient between T_m and T_c.

The crystallization process itself is strongly temperature dependent and is usually treated as a composite of two-stages: primary and secondary crystallization. Assuming the relative degree of crystallinity increases with an increase in crystallization time, t, the Avrami[37–39] equation can be used to analyze the isothermal crystallization process of Nylon 12 as a function of crystallization time and temperature as described in eq. (3):

$$X(t) = 1 - \exp(-kt^n) \tag{3}$$

A double logarithmic plot of log $[-\ln(1 - X(t))]$ versus log time was produced and is shown in Figure 3. Each plot at the individual crystallization temperature showed an initial linear character that subsequently tended to level off, indicative of the existence of a secondary crystallization stage for Nylon 12. This deviation is due to spherulite impingement in the latter stages of the crystallization process and is similar to the results reported by Liu et al. for Nylon 11.[34] The values of n (the Avrami exponent) and K (the rate parameter) were determined from the slope and intercept of the initial linear portion of the plots in Figure 3 and are listed in Table I. The Avrami exponent was in the range from 2.05 to 2.55, which according to Wunderlich[1] indicates that the mode of nucleation and growth at the primary stage of the isothermal crystallization for Nylon 12 must be complex. As the Avrami exponent is essentially greater than 2, depending on the crystallization temperature, the primary stage was concluded to be a three-dimensional growth phenomenon. The experimental crystallization data for Nylon 12 gave the closest agreement to a two-stage athermal/thermal nucleation process with branching fibrillar morphology. This method was reported to give variable fractional values of n, and it is known from previous work that Nylon 12 does produce a three-dimensional crystal structure.[40–42] The reduction in the value of n in the secondary stage of crystallization was thought to be due to the spherulites impinging on each other, similar to that discussed previously by Liu et al.[35] The form of the spherulite growth transforms into one-dimensional space extension, the crystallization mode therefore becomes simpler. Table I also lists other important parameters for this analysis, the half-time of crystallization $t_{1/2}$, which is defined as the time taken from the onset of crystallization until 50% completion which was determined from Figure 2. The relationship between the rate parameter, K, and $t_{1/2}$, is $t_{1/2} = (\ln 2/K)^{1/n}$. The dependence of $t_{1/2}$ with crystallization temperature is shown in Figure 4, and as is the case for all polymeric materials, $t_{1/2}$ increases with increasing T_c, for a relatively lower degree of supercooling. Usually the rate of crystallization, $\tau_{1/2}$ is described as the reciprocal of $t_{1/2}$, these values were used to calculate

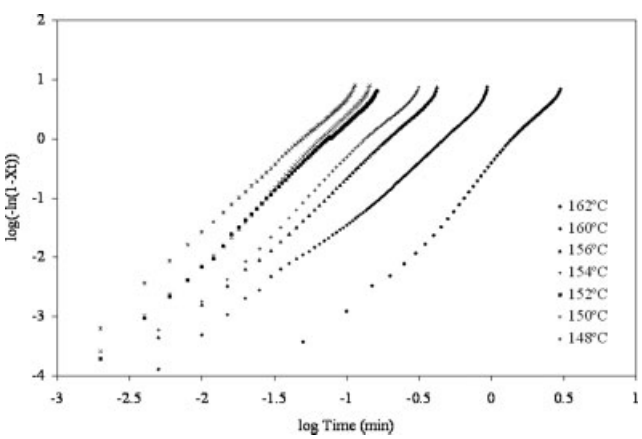

Figure 3 Avrami plot for the isothermal crystallization of Nylon 12.

TABLE I
Avrami Parameters: n, K, t_{max}, $t_{1/2}$, $\tau_{1/2}$

Temp. (K)	Temp. (°C)	$t_{1/2}$	$\tau_{1/2}$	n	K	$1/T_c$	t_{max}	$1/n \ln(K)$
435	162	1.20	0.83	2.55	0.44	0.0023	0.55	−0.33
433	160	0.40	2.50	2.05	4.54	0.0023	0.06	0.74
429	156	0.17	6.06	2.25	39.95	0.0023	0.01	1.64
427	154	0.12	8.33	2.34	98.98	0.0023	0.00	1.96
425	152	0.06	16.13	2.26	371.55	0.0024	0.00	2.62
423	150	0.06	17.54	2.47	820.00	0.0024	0.00	2.72
421	148	0.04	23.81	2.25	789.25	0.0024	0.00	2.96

the time required for maximum crystallization rate t_{max}, since this time corresponds to the point where the rate of change of heat flow rate with time is equal to zero, given by $t_{max} = [(n-1)/nK]^{1/n}$. The values of t_{max} determined are listed in Table I.

Activation energy for crystallization

The crystallization process for Nylon 12 is assumed to be a thermally activated process and the crystallization rate parameter can be approximately described by an Arrhenius type equation reported by Cebe and Hong:[43]

$$K^{1/n} = k_0 \exp -\frac{\Delta E}{RT_c} \tag{4}$$

ΔE can be determined by the slope of a plot of $1/n(\ln K)$ versus $1/T_c$. This was completed for the crystallization temperatures used in this study and is shown in Figure 5. The value of the activation energy for the primary crystallization process was determined to be −345.5 kJ/mol, in contrast Liu et al.[34] and Zhang and Mo[33] reported a value of −284.5 kJ/mol for Nylon 12,12, −394.6 kJ/mol for Nylon 11 and −485.5 kJ/mol for Nylon 6,6. The values of ΔE for Nylon 11 and 12,12 approximated more closely with the value reported for Nylon 12, but the quoted value for Nylon 6,6 was much higher, presumably as a consequence of the higher degree of hydrogen bonding between neighboring chains in Nylon 6,6. As the polymer has to release energy while transforming from the melt to the crystalline state, the value of ΔE is negative.

Turnbull–Fisher equation

To evaluate the mechanism of spherulitic growth, the Turnbull–Fisher equation[44] was used and is given as:

$$\ln G = \ln G_0 - \frac{\Delta E^*}{kT_c} - \frac{\Delta F^*}{kT_c} \tag{5}$$

where G is the spherulitic growth rate, G_0 is a pre-exponential factor, k is the Boltzmann constant, ΔE^* is the free energy of activation for transporting a chain segment from the supercooled to the crystalline phase, and ΔF^* is the free energy of formation of a crystallite nucleus of critical size. At low temperatures, the transportation term, $-\Delta E^*/kT_c$ decreases rapidly when T_c approaches T_g, the transportation term should be dominant for the crystallization rate. At high temperatures when the melt crystallization temperature approaches T_m, the nucleation term $-\Delta F^*/kT_c$ decreases rapidly,

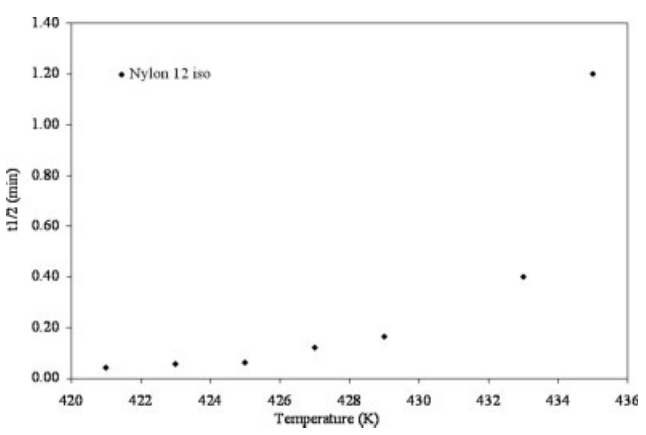

Figure 4 Plot of $t_{1/2}$ versus T_c for isothermal crystallization of Nylon 12.

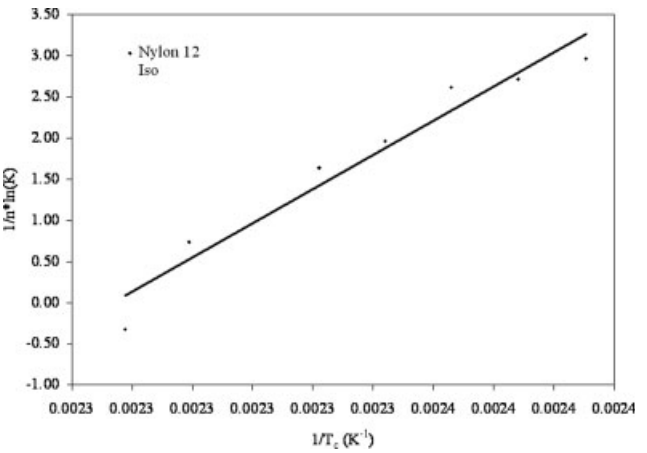

Figure 5 Plot of $1/n(\ln K)$ versus $1/T_c$ for Avrami parameter K obtained from isothermal crystallization data.

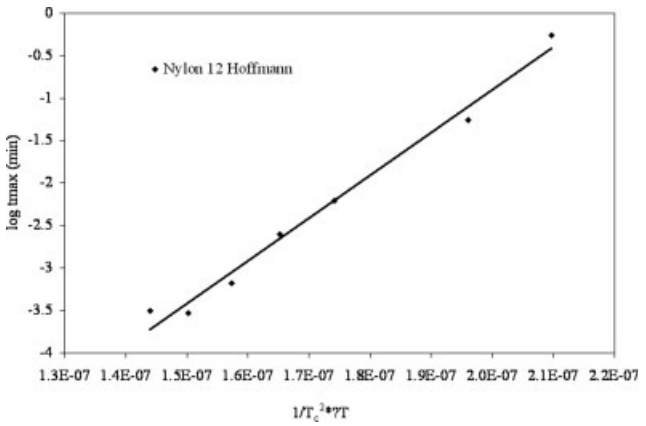

Figure 6 Plot of log t_{max} versus $1/(T_c^2\ \Delta T)$ for Nylon 12.

and it should be dominant for the crystallization rate in the melt crystallization process. This result can be explained as the presence of a maximum in the behavior of the growth rate as discussed by Ziabicki.[45] In this study the values of T_c were in the range from 435 to 421 K which approaches the Nylon 12 $T_m = 450$ K, so $-\Delta E^*/kT_c$ is negligible in the isothermal crystallization process for Nylon 12. Thus the Turnbull–Fisher equation can be simplified to:

$$\ln G = \ln G_0 - \Delta F^*/kT_c \tag{6}$$

where the crystallization rate is controlled by a single nucleation term, and the term for $-\Delta F^*/kT_c$ is adapted as derived by Hoffmann et al.[46–48] as follows:

$$\ln G = \ln G_0 - \frac{\chi T_m^0}{T_c^2(T_m^0 - T_c)} \tag{7}$$

where T_m^0 is the equilibrium melting temperature which was reported to be 460.2 K for Nylon 12 by Aharoni[49] and χ is a parameter concerned with the heat of fusion and the interfacial free energy. Lim and Llyod[50] combined the Hoffmann equation with the equation for t_{max} and the Avrami relationship to give:

$$\log t_{max} = B - \frac{C}{2.303\, T_c^2\, \Delta T} \tag{8}$$

where B and C are constants and ΔT is the degree of supercooling, i.e., $(T_m^0 - T_c)$. This relationship was used to verify that the Avrami equation adequately describes the primary stage of crystallization of Nylon 12. Figure 6 shows a plot of log t_{max} versus $1/(T_c^2\ \Delta T)$ from which t_{max} was determined and is listed in Table II. It can be seen from Figure 6 that a straight-line relationship was obtained for the primary stage crystallization of Nylon 12. The coefficient of determination of the fit of the data was found to be 0.985 and therefore Nylon 12 was undergoing primary crystallization at t_{max}.

Spherulitic growth analysis

So the Turnbull-Fisher expression would more accurately describe the crystallization process of polymers with large degrees of supercooling, Hoffman analyzed the spherulitic growth rate, G, and reported that the Lauritzen-Hoffmann et al.[46–48] equation could be rearranged to give:

$$\log G + \frac{U^*}{2.303R(T_c - T_\infty)} = \log G_0 - \frac{K_g}{2.303T_c\Delta Tf} \tag{9}$$

This allowed for a graph of $\log G + U^*/2.303R(T_c - T_\infty)$ versus $1/2.303T_c\Delta Tf$ to be plotted with a slope $= -K_g$, from which a value for K_g of 1.16×10^5 K^2 was determined, see Figure 7. The value of K_g for Nylon 12 allowed the apparent lateral and end surface free energies, σ and σ_e to be calculated using either of the following formulas:

$$K_g(I) = \frac{4b_0(\sigma\sigma_e)T_m^0}{\Delta H_f^0 k} \tag{10}$$

$$K_g(II) = \frac{2b_0(\sigma\sigma_e)T_m^0}{\Delta H_f^0 k} \tag{11}$$

where b_0, is the thickness of a monomolecular layer in the crystal, k is the Boltzmann constant and ΔH_f^0

TABLE II
Data for Turnbull-Fisher Plot

Temp. (K)	Temp. (°C)	t_{max}	T_c^2	ΔT	$1/(T_c^2\Delta T)$	Log t_{max}
435	162	0.54744	189225	25.2	2.1 E−07	−0.2617
433	160	0.05509	187489	27.2	1.96 E−07	−1.2589
429	156	0.00618	184041	31.2	1.74 E−07	−2.2089
427	154	0.00247	182329	33.2	1.65 E−07	−2.6069
425	152	0.00066	180625	35.2	1.57 E−07	−3.1779
423	150	0.00029	178929	37.2	1.5 E−07	−3.5319
421	148	0.00031	177241	39.2	1.44 E−07	−3.5047

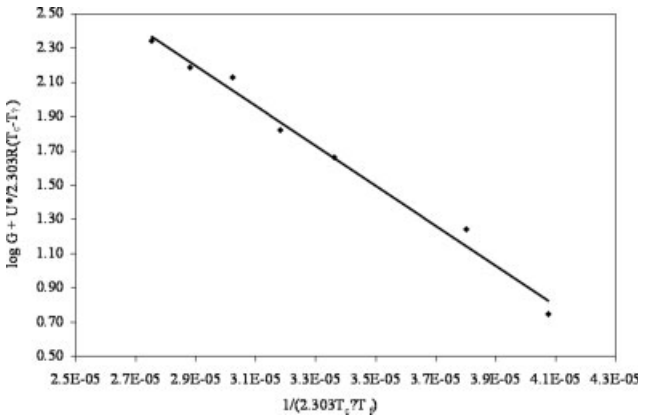

Figure 7 Hoffmann plot for isothermal crystallization of Nylon 12.

is the bulk enthalpy of fusion per unit volume for a fully crystalline polymer and can be expressed as $\Delta H_f^0 = \Delta H_m^0\ \rho_c$. Gogolewski quoted ΔH_m^0 as being 209.2 J/g[51] and Chuah et al.[52] quoted ρ_c to be 1.04, therefore $\Delta H_f^0 = 217.6 J/g$. For Regime I kinetics the formation of a surface nucleus is followed by rapid completion of the substrate. In contrast, for Regime II kinetics the surface nuclei form in large numbers from the substrate and spread slowly. To investigate what Regime growth Nylon 12 exhibited the *Z*-test described by Lauritzen and Hoffmann[53] was employed. *Z* is defined by:

$$Z \equiv 10^3 (L/2a_0)^2 \exp[-X/T_c(\Delta T)] \tag{12}$$

where *L* is the effective lamellar width and a_0 is the width of the molecular chain in the crystal. Substitution of $X = K_g$ into the *Z*-test initially proposed by Avrami yields $Z \leq 0.01$, the crystallization conforms to Regime I kinetics. On the other hand, if $X = 2K_g$, substitution into the *Z*-test yields $Z \geq 1$, regime II kinetics are apparent. It was considered more convenient, as reported by Lauritzen and Hoffmann[54] to use the calculated value of K_g and the inequalities for *Z* discussed above to estimate the range of values of *L* dependent on crystallization temperature in both regime I and II type kinetics and determine their validity. The Bavais–Friedal standards discussed by Hoffmann and Miller[48] were applied, which state that the preferred face will be the crystal plane with the largest spacing. Therefore, as described previously by Aharoni[49] Nylon 12 exhibits the stable γ-modification with monoclinic hexagonal unit cells, with the lattice cell parameters being a = 0.958 nm, b (chain direction) = 3.19 nm, and c = 0.479 nm. The unit-cell angles are $\alpha = \gamma = 90^\circ$ and $\beta = 120^\circ$, and there are four monomeric repeat units in each unit cell. The thickness of a monomolecular layer b_o in the preferred growth chain is 0.42 nm and the chain width a_0 is 0.479 nm.[51] Assuming $Z \leq$ 0.01 and after substitution of $X = K_g$ into the *Z*-test it was found that *L* was in the range of 1.90–3.22 nm, in reasonable agreement for Nylon 12. Assuming $Z \geq 1$ and $X = 2K_g$ it was calculated that *L* was in the range 190–32.2 nm which is unrealistic when compared with studies completed by Liu and Zhang on Nylon 11[34] and Nylon 6,6,[33] respectively. It is apparent that crystallization of this Nylon 12 follows regime I type kinetics; that is numerous surface nuclei are involved in the formation of the substrate and the regime I eq. (10) stated previously is now applicable.

Surface-free energy (σ, σ_e) and work of chain folding (q)

In accordance with the procedure discussed by Hoffmann et al.,[46,47] σ and σ_e were determined from the value of $\sigma\sigma_e$ using the following equation:

$$\sigma = \alpha \Delta H_f^0 (a_0 b_0)^{1/2} = \alpha \Delta H_f^0 (A_0^{1/2}) \tag{13}$$

where A_0 is the cross-sectional area of a chain in the crystal, and α is an empirical constant which usually ranges between 0.1 and 0.3. In general α = 0.1 for polyolefins, 0.24 for polyesters, and 0.3 for most organics. The three values of α quoted above were used to compare the results to find out which one (if any) produced more reasonable results for the Nylon 12 of interest. The values of σ calculated with α = 0.24 and 0.3 were unrealistically small, as the value of σ was calculated to be 9.38 erg/cm^3. σ_e was then calculated using the equation for regime I kinetics, [eq. (10)], giving a value of 48.03 erg/cm^3.

The work of chain folding per molecule fold was obtained using further theory described by Hoffmann et al.:[46]

$$\sigma_e = \sigma_e^0 + \frac{q}{2a_0 b_0} \tag{14}$$

where σ_e^0 is the value of σ_e assumed if no work is required to form the fold, and q is the work required to bend a polymer chain back upon itself taking into account the conformational constraints imposed on the fold by the crystal structure. Hoffmann[46,47] reported that σ_e^0 may be set as zero, and accordingly the above equation can be rewritten as:

$$q = 2a_0 b_0 \sigma_e \tag{15}$$

For any single polymer σ_e is considered to be inversely proportional to the chain area ($a_0 b_0$), with the proportionality constant being $q/2$, therefore q was calculated to be 1.93 E−20 J per molecular chain fold or by dividing by Avagadros number q = 11.7 kJ/mol for this grade of Nylon 12. In comparison

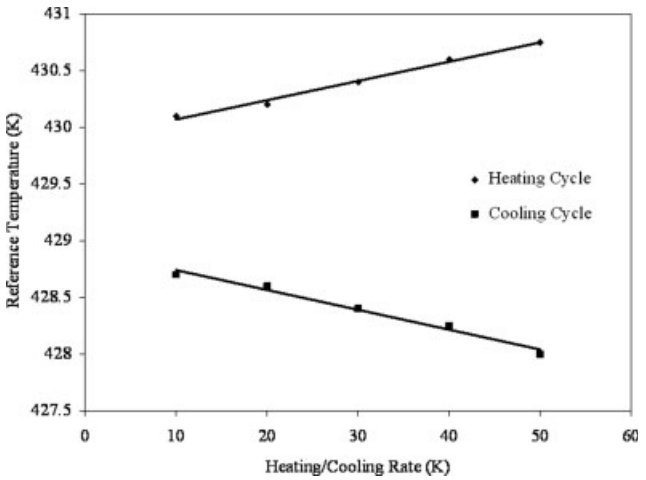

Figure 8 Calibration curves for the DSC VI at various scan rates using pure indium.

Zhang and Mo[33] and Liu et al.[34] obtained values for Nylon 6,6 (q = 33.14 kJ/mol), Nylon 11 (7.61 kJ/mol) and Nylon 10,10 (3.96 kJ/mol), thus the polymer chains of this grade of Nylon 12 were not as stiff as those in Nylon 6, 6, but were stiffer than those for Nylon 11 and Nylon 10, 10.

Nonisothermal crystallization

Temperature correction

In nonisothermal experiments, the recorded temperatures of the sample must be corrected to account for the thermal lag between the calorimeter furnaces at any given time.[12] Thermal lag is the sum of the thermal gradient inside the sample and of the temperature lag between the sample bottom and the calorimeter furnace. Monasse and Haudin[55] investigated the thermal gradient for a 300-μm thick sample of polypropylene (PP) using a finite difference method taking into account the geometry, thermal conductivity, heat capacity and crystallization kinetics of the PP sample. Their model gave a 1 K maximum gradient inside the sample during an 80 K/min cooling cycle. For a cooling rate of 50 K/min the temperature lag between the sample bottom and calorimeter furnace was found to be 4.5 K. It was therefore considered that Nylon 12 has a small thermal gradient since the DSC samples used in this study were not thicker than 300 μm, only the temperature lag will be considered in the nonisothermal study. Figure 8 shows a plot of the measured melting and solidification temperatures of pure indium samples at various scanning rates up to 50 K/min. A trend-line was used to fit the data and the following relationship was used to correct for the effect of temperature lag on the measured nonisothermal temperatures:

$$T_{\text{actual}} = T_{\text{disp}} + 0.0168\lambda \quad (16)$$

where T_{disp} is the display temperature and λ (K/min) is the cooling or heating rate set during the DSC run.

DSC measurements

In Figure 9 the full DSC melting and crystallization uncorrected endotherms recorded by the Pyris software can be seen for eight different cooling rates. From the DSC melting endotherms recorded for this study at a heating rate of 20 K/min, the average melting onset temperature, $T_{m\text{on}}$, peak melting temperature, T_m and melting offset temperature, $T_{m\text{off}}$ were recorded as 423, 448, and 454 K, respectively. There was a tolerance of ±1 K between these three temperatures for the seven tests completed, which was within acceptable tolerance for the purpose of this study. The samples were heated to 493 K and held for 10 min at that temperature to ensure complete melting of any residual crystalline content of the polymer. The corrected crystallization endotherms both as a function of temperature and time are shown in Figures 10 and 11, respectively. It was found that when the cooling rate was increased, this caused the crystallization onset temperature T_{con}, peak crystallization temperature, T_c and crystallization offset temperature, T_{coff} to be shifted to lower temperatures. Conversely, this caused the time taken for onset, peak, and offset crystallization temperatures to be reached to decrease, as shown in Figure 10. To convert the data shown in Figure 9 to a time dependent scale the following relationship between temperature, T and time, t was used:

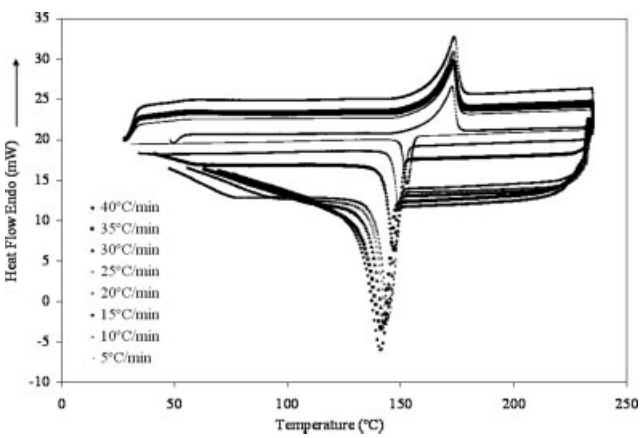

Figure 9 Melting and crystallization isotherms of Nylon 12 recorded for cooling rates of 5–40 K/min as a function of temperature.

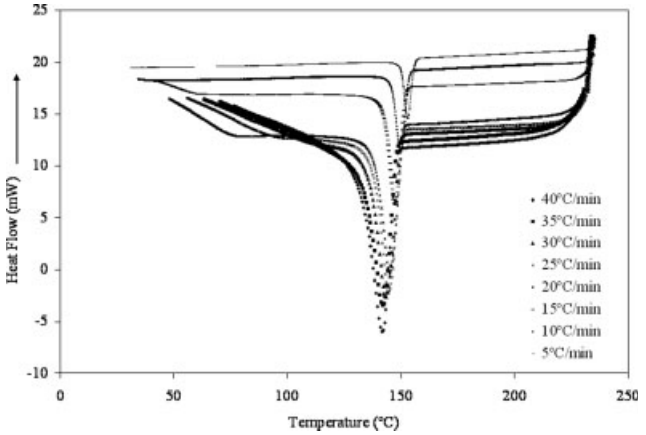

Figure 10 Crystallization endotherms of Nylon 12 recorded for cooling rates of 5–40 K/min as a function of temperature.

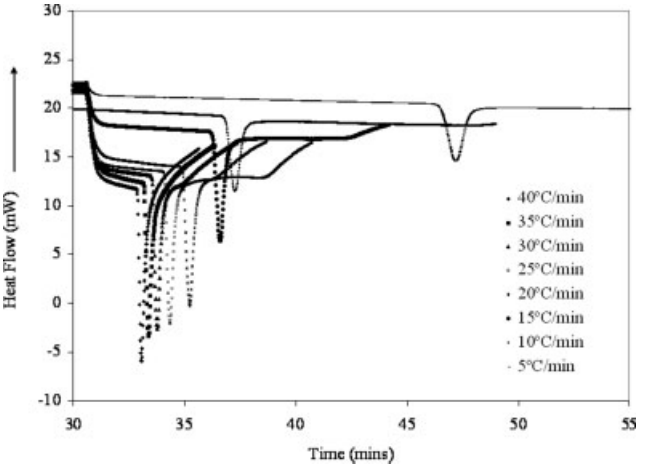

Figure 11 Crystallization endotherms of Nylon 12 recorded for cooling rates of 5–40 K/min as a function of time.

$$t = \frac{[T_{con} - T]}{\lambda} \tag{17}$$

T is the current temperature in the scan after T_{con}. The scaled crystallization profile shown in Figure 10 was used in conjunction with eq. (17) to produce Figure 11. The data also indicated that for each cooling rate, very different rate dependencies existed in the melt crystallization kinetics for Nylon 12, the values of T_{con}, T_c, T_{coff}, time for 50% of crystallization to occur from the onset time, ($t_{1/2}$), and enthalpy of crystallization to occur are listed in Table III. The rate dependence of T_c and T_{coff} can be discussed by examining the time available for crystal growth. The higher cooling rates, i.e., >25 K/min, meant that crystallization of the sample occurred over a much shorter period of time, shown by the values of $t_{1/2}$ listed in Table III. The temperature range that crystallization occurs was found to have a similar trend dependent of cooling rate, again obvious from the values listed in Table III. The slower cooling rates allowed for better development of the crystal structure in Nylon 12 as a consequence of the sample having a longer hold time within the crystallization temperature range compared to scans recorded at a higher rate. From the DSC cooling endotherms, information on the values of relative crystallinity as a function of both temperature and time were determined. The percentage crystallinity of the sample, $X(T)$, was calculated by the integration of the crystallization endotherms using the least squares method at specific intervals of temperature. The relative crystallinity $X(T)$ was then obtained by taking the quotient of the total number of squares under the curve and the number of squares between T_{con} and the specified temperature for that cooling rate. Therefore, a range of values of $X(T)$ between T_{con} and T_{coff} for each cooling rate was converted to $X(t)$, see Figure 12. It can be seen in Figure 11 that for larger cooling rates crystallization occurs rapidly, in agreement with the values obtained for $t_{1/2}$ listed in Table III. A similar plot was found when a graph of $X(T)$ versus temperature was produced and is shown in Figure 13, and for both Figures 12 and 13 a series of *S*-shaped curves were obtained. In the primary crystallization region, i.e., below $X(T) = 0.8$, the rate of crystallization is high as shown by the steepness of the gradient of the curve in this region. Above $X(T) = 0.8$ the rate of crystallization then slows and the curve plateaus, the curves finally having a distinctive sigmoidal (S) shape. At higher cooling rates, the transition between the primary and secondary crystallization regions is

TABLE III
Rate Dependent Parameters Determined for Nonisothermal Crystallization

Cooling rate (K/min)	T_{con} (K)	T_{coff} (K)	T_c (K)	$t_{1/2}$ (min)	ΔH_c (J/g)	X_c (%)
40	422.3	386.3	414.4	0.39	50.3	24.8
35	423.8	387.8	415.4	0.42	59.1	29.1
30	424.1	388.1	416.1	0.47	46.8	23.1
25	425.1	389.2	417.7	0.53	46.9	23.1
20	426.1	390.7	417.7	0.61	53.0	26.1
15	427.9	392.1	420.3	0.70	39.5	19.5
10	430.5	394.0	422.8	0.84	37.1	18.3
5	433.8	398.6	425.8	1.55	43.4	21.4

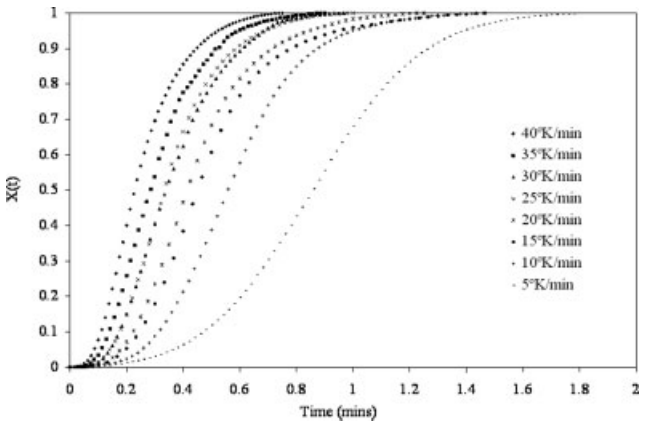

Figure 12 Change of relative crystallinity $X(t)$ as a function of time.

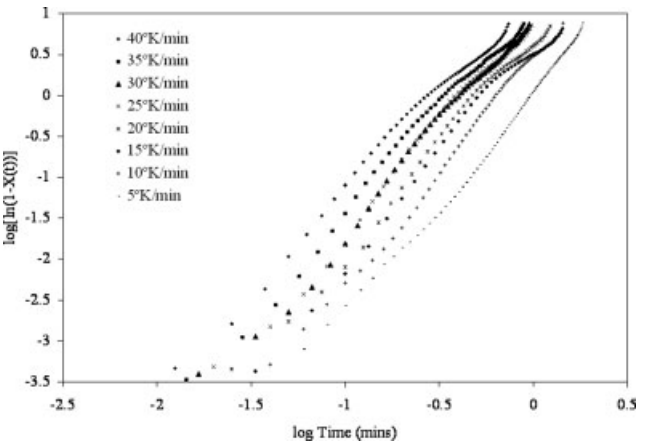

Figure 14 Jeziorny plot of log $\{-\ln(1 - X(t))\}$ versus log time for the nonisothermal crystallization process of Nylon 12.

less pronounced, however it is clear that there was a change in the crystallization rate. This change in rate has been attributed to spherulite impingement, previously described by Wunderlich and Poisson.[1,3] They reported the primary growth stage to continue unrestricted until a point where the individual crystals begin to touch and therefore restrict their rate of growth. To more accurately describe the mechanism of the stages of crystallization experienced by Nylon 12, a number of models have been developed to describe the nonisothermal crystallization kinetics of polymers. Their applicability to the Nylon 12 used in this study was investigated using the following:

1. Jeziorny extended Avrami equation;
2. Ozawa equation;
3. Cazé Average Avrami exponent;
4. Chee Average Avrami exponent;
5. Combined Avrami/Ozawa Equation;
6. Kissinger activation energy.

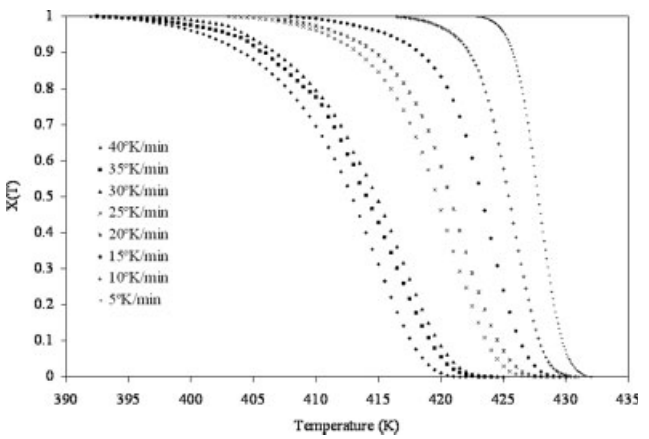

Figure 13 Change of relative crystallinity $X(T)$ as a function of temperature.

Jeziorny-modified Avrami equation[56]

Mandelkern[57] considered that the primary stage of the nonisothermal crystallization can be described by the Avrami equation based on the assumption the crystallization temperature is constant. Jeziorny assumed that cooling rate was constant or approximately constant. The final form of the rate parameter characterizing the kinetics of nonisothermal crystallization can thus be given as:

$$\log Z_c = \log \frac{Z_t}{\lambda} \tag{18}$$

From eq. (18), a plot of log $[-\ln(1 - X(t)]$ versus log time will yield the values of the Avrami exponent, n and the rate parameter Z_c or Z_t from the slope and the intercept of the graph, as shown in Figure 14. It was evident that a two-stage crystallization process exists for Nylon 12, similar to data reported by Liu et al.[34] for Nylon 11, and the crystallization process can be divided into primary and secondary stages, the values of n, Z_t, and Z_c for both stages are listed in Table IV. At the primary stage of crystallization the Avrami exponent, n_1 varies from approximately 2.3 to 2.9. This indicates that the mode of nucleation and growth at the primary stage of the nonisothermal crystallization for Nylon 12 is complex. As the Avrami exponent is essentially greater than 2, dependent on the cooling rate, the primary stage was concluded to be a three-dimensional growth phenomenon, in agreement with the theory proposed by Wunderlich.[1] The experimental crystallization data for Nylon 12 gave the closest agreement to the two-stage athermal/thermal nucleation process with branching fibrillar morphology. This method was reported to give variable fractional values of n, and it is known from previous work that Nylon 12 does produce a three-dimensional

TABLE IV
Values of n, Z_t, and Z_c from the Jeziorny-Modified Avrami Equation for the Two-Stages of Nonisothermal Crystallization of Nylon 12

λ (K/min)	Log λ	n_1	n_2	Log Z_{c1}	Log Z_{t1}	Log Z_{c2}	Log Z_{t2}
40	1.602	2.666	1.82	1.563	0.039	1.010	0.025
35	1.544	2.764	1.90	1.367	0.265	0.902	0.026
30	1.477	2.729	1.93	1.075	0.242	0.807	0.027
25	1.398	2.802	2.20	1.143	0.328	0.859	0.034
20	1.301	2.796	1.85	0.861	0.343	0.623	0.031
15	1.176	2.943	1.52	0.819	0.192	0.514	0.034
10	1.000	2.531	2.12	0.242	0.118	0.467	0.047
5	0.699	2.363	2.77	−0.234	−0.139	0.079	0.016

crystal structure.[40–42] The reduction in the value of n_2 to around 1.8 to 2.7 compared to n_1 is due to the spherulites impinging on each other, again similar to that discussed by Liu for Nylon 11.[58] The form of spherulite growth transforms into one-dimensional space extension, the crystallization mode therefore becomes simpler. The wide variation in the calculated values of n makes it difficult to assign an average value of n. However, a method devised by Ozawa[59] will be discussed in the next section that has been specifically designed to model nonisothermal crystallization kinetics by modeling the change in $X(T)$ as a function of cooling rate.

Ozawa analysis

A method of modeling the nonisothermal crystallization kinetics was derived by Ozawa,[59] by extending the Avrami equation such that the Avrami model is modified to allow for all the processes of nonisothermal crystallization. A graph of ln $[-\ln(1 - X(T))]$ versus log λ was constructed from data points taken at different temperatures in the range 428–410 K during the crystallization process and is shown in Figure 15. Ozawa reported that his treatment showed good agreement modeling the crystallization behavior of PET, shown by a series of parallel straight lines constructed in the range of crystallization temperatures. However, the data in Figure 15 suggests that this method cannot be used to describe the crystallization kinetics of Nylon 12, as similar to the Jeziorny modified Avrami model a clear two-stage process of crystallization was found to exist. This also agrees with the findings of Liu et al.[34] who reported that the Ozawa treatment does not predict the crystallization behavior of Nylon 11. Further evidence of the limitations of the Ozawa model and its application to nonisothermal crystallization kinetics is evident from the data listed in Table V. Values of m_1, m_2, (Ozawa exponents) ln $K(T)_1$ and ln $K(T)_2$ are listed and the data shows in agreement with the results obtained previously using the Jeziorny treatment, the values of the Ozawa exponent, m, are quite scattered. The scatter of m was understandable as nonisothermal crystallization is a dynamic process in which the crystallization rate is no longer constant, but a function of time and cooling rate. The strong dependence of cooling rate on the mechanism of crystal growth for Nylon 12 in the primary stage of crystallization is such that the value of m_1 has a large tolerance. As spherulite impingement slows down crystal growth in the secondary crystallization stage, the values of m_2 were reduced and with smaller variance. It was concluded that the Ozawa equation did not satisfactorily describe the nonisothermal crystallization kinetics of Nylon 12. The Ozawa plot showed a clear two-stage process with

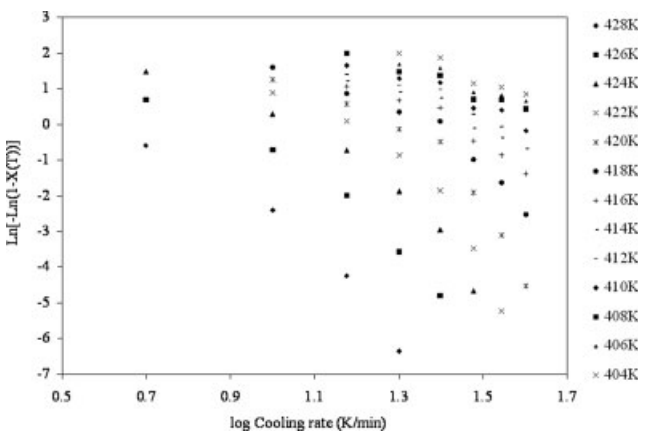

Figure 15 Ozawa plot of log$[-\ln(1 - X(T))]$ versus log λ for Nylon 12.

TABLE V
Ozawa Paramters for a Two-Stage Crystallization Process

Temp. (K)	m_1	m_2	Ln K $(T)_1$	Ln K $(T)_2$
428	−12.95	−7.47	10.68	4.73
426	−12.67	−5.51	12.31	4.61
424	−12.65	−5.38	14.37	5.41
422	−17.92	−5.73	22.77	6.68
420	−19.55	−4.57	26.92	5.80
418	−12.47	−4.15	17.51	5.75
416	−8.82	−3.20	12.71	4.84
414	−6.74	−2.48	10.61	4.15
412	−5.70	−2.40	8.85	4.23
410	−6.08	−2.15	9.62	5.15

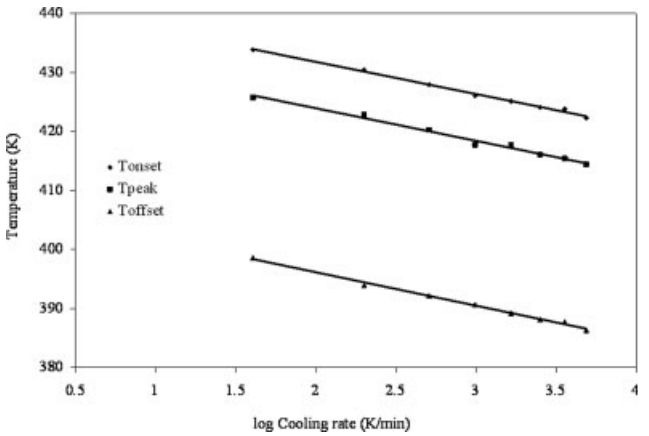

Figure 16 Evolution of T_{con}, T_c and T_{coff} for Nylon 12 as a function of cooling rate.

two values of m, (m_1 and m_2). Ozawa[59] reported that for the equation to be valid only one value of m should exist. Ozawa ignored secondary crystallization and López et al.[25] argued that during cooling secondary crystallization can be neglected as the temperature is lowered continuously. The data presented in Figure 15 confirms that the latter assumption is not valid for Nylon 12. It is quite clear that crystal impingement has a clear effect on the dependence of $X(T)$ with time and temperature and a method which accounts for this is required to correctly model the kinetics of Nylon 12.

Cazé average Avrami exponent

The method reported by Cazé[60] is a relatively simple method by which an average value for the Avrami exponent, n, can be determined based on experimental measurements from DSC cooling curves of the three temperature inflection points, T_{con}, T_c, and T_{coff} at varying cooling rates. According to this theory these temperatures vary linearly with cooling rate. Using this technique a plot of inflection temperature versus ln cooling rate was produced for the crystallization behavior of Nylon 12 and is shown in Figure 16. It is evident there is good agreement between the application of the method reported by Cazé and the data obtained from the Nylon 12 endotherms. The values for the following constants were obtained; $A = -5.5$, $B_1 = 407.05$, and $B_2 = 442.73$. Using these values n was calculated to be 0.292, different from the range of values of n generated using the Jeziorny modified Avrami method. The data reported by Liu et al.[35] using the Cazé average Avrami exponent suggested that this method was successful in producing a valid value of n for Nylon 12,12. However, similar to the previous methods discussed this does not take into account secondary crystallization, therefore, an average was taken of the value of n for both stages of crystallization, not just the primary stage. Furthermore, the value of T_{coff} is subjective as it is difficult to accurately assign, especially when secondary crystallization occurs, like in the case of Nylon 12. It was concluded that the secondary crystallization process, taking place over a longer period of time reduces the value of T_{coff} thus giving an incorrect value of n for Nylon 12. The use of this method to predict n for a two-stage crystallization process like that exhibited by Nylon 12 is questionable. The validity of this model is further called into question by the subjective nature of the assignment of a value of T_{coff} as there may be a temptation to cite a lower value of this temperature so as to produce a better value of n. A more applicable method to calculate the average value of n, for the primary stage only, was developed by Chuah.[52]

Chuah method for average Avrami exponent

This method is based on the Ozawa equation, in that it determines the Avrami exponent (n) using data exclusively from the primary crystallization regime, and Chuah reported that the method may be used to account for shortcomings in both the Ozawa and Cazé methods. From the DSC endotherms the weight fraction of the crystal structure and volume fraction X_v can be calculated using equation:

$$X_v(T) = \frac{X_w(T)\frac{\rho_a}{\rho_c}}{1 - \left[1 - \frac{\rho_a}{\rho_c}\right]X_w(T)} \tag{19}$$

To account for the temperature effects on the ratio ρ_a/ρ_c the empirical rules reported by Boyer-Spencer-Bondi[61] were used. They quoted $\alpha_a T_g = 0.17$ and $\alpha_c T_m^0 = 0.11$ where α_a and α_c are the thermal expansion coefficients of the amorphous and crystalline regions of the polymer, T_g and T_m^0 are the glass transition and equilibrium melting temperature respectively. The value of T_g for this grade of Nylon 12 was taken as 313 K and the value of T_m^0 was reported by Pfliiger[62] to be 460.2 K. Equation 20 was then used to evaluate the ratio of ρ_a/ρ_c for Nylon 12:

$$\frac{\rho_a}{\rho_c} = \left(\frac{\rho_{ao}}{\rho_{co}}\right)\exp\left[(T - T_r)\left(\frac{0.11}{T_m^0} - \frac{0.16}{T_g}\right)\right] \tag{20}$$

where o refers to the properties at the reference temperature, the values of ρ_{ao} and ρ_{co} are reported by Pfliiger as 1.01 and 1.04, respectively, and T_r (reference temperature) was taken as 298 K in this case. Using eqs. (19) and (20), Chuah proposed that the equations:

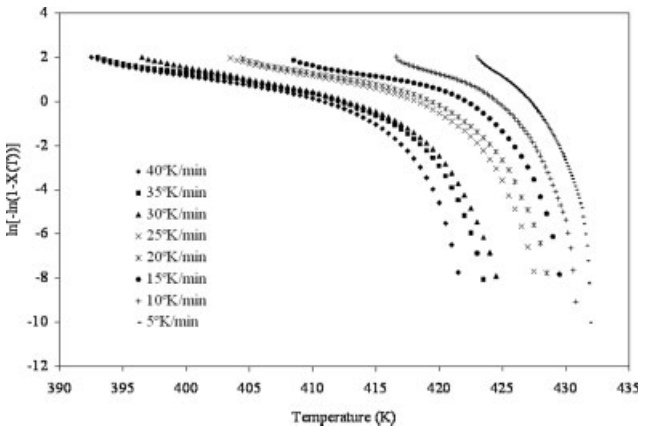

Figure 17 Chuah plot of ln $[-\ln(1 - X_v)]$ versus temperature for various cooling rates.

$$\ln K^*(T) = a(T - T_1) \tag{21}$$

$$K^*(T_\lambda) = \lambda^n \tag{22}$$

could be used as a basis to describe the primary crystallization stage of Nylon 12. A plot of ln $[-\ln(1 - X_v)]$ versus T was produced using the theory discussed, the constants a and aT_λ being the gradient and intercept of the graph respectively, see Figure 17. It's evident from these results that a two-stage crystallization process exists for Nylon 12. The curves in Figure 17 were separated to only show the primary stage of the crystallization, as shown in Figure 18. From this relationship a plot of ln λ/a versus T_λ for the seven cooling rates studied was plotted. Ozawa reported that the rate parameter $K(T)$ is a function of the temperature of the onset of crystallization, thus it can be assumed that the parameter, a is virtually cooling rate dependent and n can be calculated from the slope of the linear plot. The data used to construct this plot is listed in Table VI, from which a graph of ln λ/a versus T_λ was produced and good agreement was achieved with the Chuah model, see Figure 19. A R^2 value of 0.95 was recorded when a linear trend line was fitted to the data points and $n = 5.46$ obtained from the slope of the line in Figure 19. This is a higher value than the $n = 1.57$ recorded by Chuah for a different grade of Nylon 12 and the value of n recorded for the primary stage of crystallization using the Jeziorny treatment. However, reasonable agreement was achieved between the calculated value of n and that reported by Maneschalchi[63] of $n = 5.06$ for Nylon 12 scanned isothermally. The value of n shows a pronounced difference between the dynamic and quiescent crystallization kinetics, the former yields a slower rate and the value of n can be linked to the growth of a two-stage process with fibrillar morphology, as discussed by Wunderlich,[1] in agreement with the observations drawn from the Jeziorny treatment of the data. The Chuah method confirmed the behavior predicted using the Jeziorny modified Avrami treatment. The mechanism of crystal growth for Nylon 12 when it undergoes nonisothermal crystallization can be assigned as an athermal/thermal nucleation two-stage crystallization process with branching fibrillar morphology. However, this method does not allow for 100% certainty in the interpretation of the exponent n, without complementary information on the morphology and crystallization mechanism.

TABLE VI
Chuah Parameters used for Calculation of Average Avrami Exponent (n)

λ (K/min)	a	$aT\lambda$	$T\lambda$	Ln λ/a
40	−1.33	−554.03	416.56	−2.77
35	−1.44	−600.60	418.25	−2.48
30	−1.43	−599.93	419.53	−2.38
25	−1.53	−645.60	422.65	−2.11
20	−1.58	−667.96	423.81	−1.90
15	−1.88	−798.53	425.59	−1.44
10	−2.35	−1002.70	426.68	−0.98
5	−3.45	−1481.90	429.54	−0.47

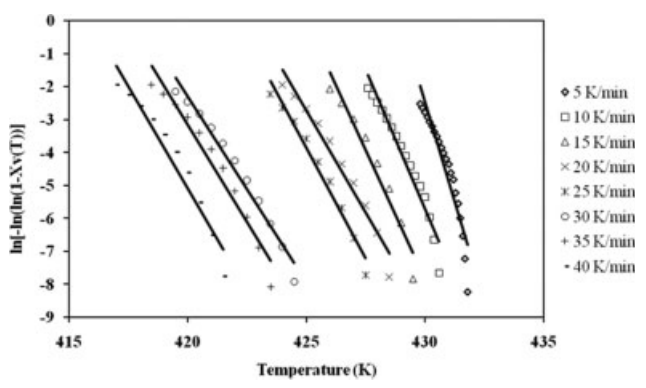

Figure 18 Chuah plot of ln $[-\ln (1 - X_v)]$ versus temperature for the primary crystallization stage.

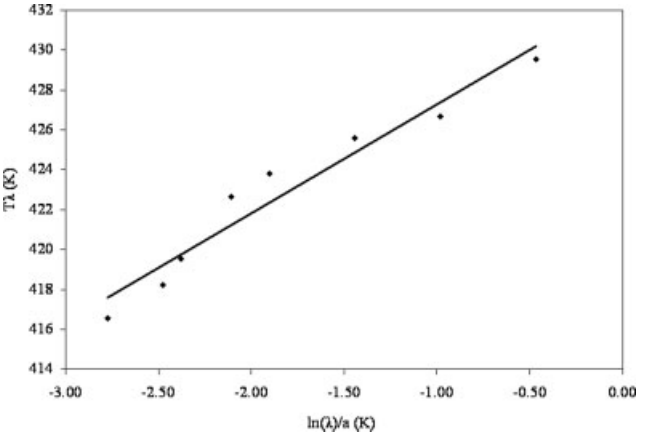

Figure 19 Chuah plot of T_λ versus ln λ/a for Nylon 12.

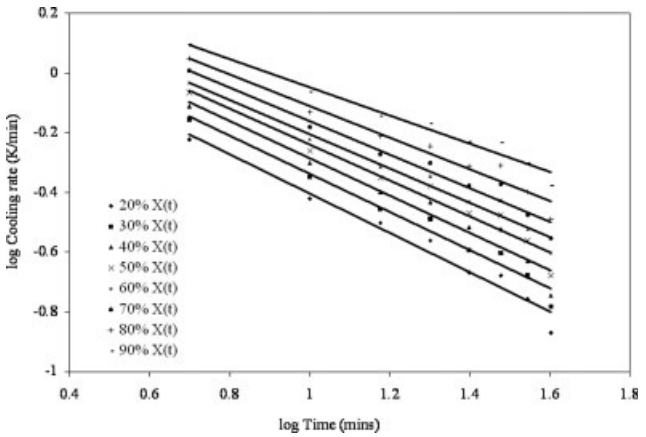

Figure 20 Combined Avrami/Ozawa plots for Nylon 12.

This modification of the Ozawa equation is a useful tool for describing the dynamic crystallization behavior of polymers. More importantly, it provided a practical means of assessing the Avrami exponent reliably over a wide range of relative undercoolings.

Combined Avrami and Ozawa equation[64]

It is evident from the models discussed previously that they do not consider the importance of the secondary stage of nonisothermal crystallization, by only describing the primary stage of crystallization. To completely describe the nonisothermal crystallization process of Nylon 12 the model reported by Mo et al.,[64] which combines the Avrami and Ozawa equations was used to treat the Nylon 12 endotherms obtained. Liu et al. reported this method successfully dealt with the nonisothermal crystallization behavior of Nylon 11.[64] For a given value of $X(t)$, a plot of log cooling rate versus log time, (which in this case is the time taken for T_{con} for $X(t)$ to reach 100%), was produced for values of $X(t)$, 20, 30, 40, 50, 60, 70, 80, and 90%. The values of b and $F(T)$ for a certain value of $X(t)$ were determined from the slope and the intercept of the best fit trend-line drawn through the data points for each cooling rate at the assigned value of $X(t)$, see Figure 20. It was evident that there was good agreement between the Liu analysis and the experimental data for Nylon 12, as the values of R^2, the coefficient of determination for the trend-lines, were in excess of 0.96 for each plot at the assigned value of $X(t)$. The values of b, $F(T)$ and the coefficient of determination for each value of $X(t)$ are listed in Table VII. In agreement with that reported by Liu, the values of $F(T)$ systematically increased with rising relative crystallinity, indicating that at a unit crystallization time, a higher cooling rate should be used to obtain a higher degree of crystallinity. Liu et al.[34] and Mo[64] both stated that the values of b remained almost constant,

TABLE VII
Values of b and $F(T)$ as a Function of $X(t)$

$X(t)$	b	Log $F(T)$	$F(T)$	R^2
90	0.472	0.425	2.661	0.970
80	0.530	0.420	2.630	0.961
70	0.562	0.401	2.518	0.965
60	0.575	0.370	2.344	0.970
50	0.602	0.363	2.307	0.956
40	0.625	0.340	2.188	0.951
30	0.639	0.302	2.004	0.973
20	0.659	0.255	1.799	0.969

independent of the value of $X(t)$. The values listed in Table VII did not support this conclusion for this Nylon 12, as there was a definite trend in which the values of b decreased as the value of $X(t)$ increased. This change in the exponent b is determined by the time taken for crystallization to reach completion, i.e., $X(t) = 1$. In Figure 20 it can be seen that the slower cooling rates result in a longer time over which crystallization occurs, conversely, increasing the cooling rate reduces the time of crystallization. When the values of log time are taken at the specific values of $X(t)$ it was found that there was a wide spread of log T at the higher cooling rates, which then narrowed as the cooling rate was decreased. This causes an increase in the value of b indicating b can also be considered strongly cooling rate dependent. In support of this conclusion a plot of exponent b versus $X(t)$ and log $F(T)$ versus $X(t)$ were produced, as shown in Figures 21 and 22, respectively. The data in Figure 21 supports the conclusion that b is strongly cooling rate dependent, in that a linear equation of the form $b = AX(t) + C$ was found to exist between the exponent, b and $X(t)$. For this grade of Nylon 12, A and C were found to be -0.0025 and 0.7185, respectively. Figure 22 also showed a linear relationship, this time of the form, log $F(T) = DX(t) + E$, also existed for the rate parameter, $F(T)$. D and E were found to be 0.002 and 0.231, respectively.

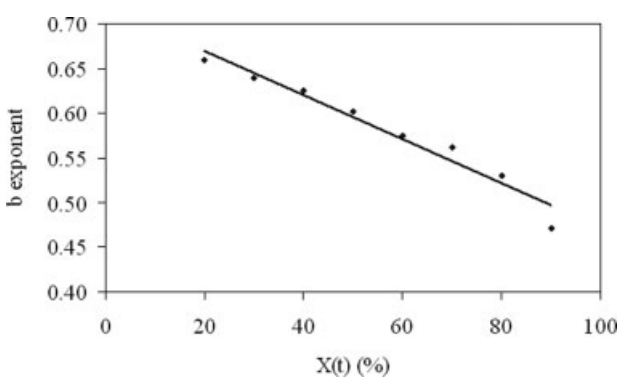

Figure 21 Exponent b versus $X(t)$ for combined Avrami/Ozawa treatment.

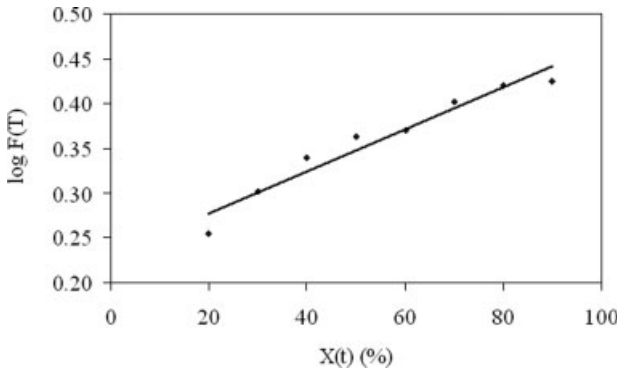

Figure 22 Log $F(T)$ versus $X(t)$ for combined Avrami/Ozawa treatment.

Kissinger activation energy (ΔE)

Accounting for the influence of varying cooling rates in the nonisothermal crystallization process, Kissinger[65] reported the activation energy could be determined based on the following equation:

$$k_T = A \exp\left(\frac{-E}{RT}\right) \tag{23}$$

As the temperature changes so does the rate of crystallization, the maximum value of the reaction rate during crystallization occurs at T_c and the derivative at that point with respect to time is zero. Kissinger therefore determined the activation energy, ΔE, using the following equation:

$$A \exp\left(\frac{-E}{RT_c}\right) = \frac{E}{RT_m^2}\frac{dT}{dt} \tag{24}$$

which can be rewritten as:

$$\frac{d\left[\ln\left(\frac{\lambda}{T_c^2}\right)\right]}{d\left(\frac{1}{T_c}\right)} = -\frac{\Delta E}{R} \tag{25}$$

where $\frac{dT}{t} = \lambda$ is the cooling rate. A plot of $\ln \lambda/T_c^2$ versus $1/T_c$ was produced, see Figure 23, and $\Delta E/R$ determined from the slope of the best fit trend-line of this plot As the polymer has to release energy while transforming from the melt to the crystalline state, the value of ΔE is negative on the basis of the concept of heat quantity in physical chemistry. The individual values of $1/T_c$ dependent on cooling rate were found to show good agreement in this study. The Kissinger activation energy for the nonisothermal crystallization of Nylon 12 was found to be −293 kJ/mol. Zhang and Mo[33] and Liu et al.[34] calculated the activation energy using the Kissinger method for Nylon 66 and Nylon 11 using a similar range of cooling rates. They reported values of −331 and −328 kJ/mol for Nylon 66 and 11, respectively, somewhat similar to that calculated for the Nylon 12 used in this study.

CONCLUSIONS

The Avrami equation was used to study the isothermal crystallization kinetics of Nylon 12 and an Avrami exponent (n) in the range 2.05 to 2.55 was determined. The primary stage of Nylon 12 crystallization follows a three-dimensional growth mechanism and crystallizes via a two-stage athermal/thermal nucleation process with branching fibrillar morphology. The value of the activation energy for the primary crystallization process was found to be −345.5 kJ/mol., slightly above that reported for Nylon 12,12 (−284.5 kJ/mol).[34] It was evident from a Turnbull-Fisher plot that at t_{max} Nylon 12 is still undergoing primary crystallization. The apparent lateral (σ) and end surface (σ_e) free energies were calculated using the Hoffman equation and from the values obtained using the Lauritzen Z-test (σ = 9.38 erg/cm^3; σ_e = 48.03 erg/cm^3) it was concluded that during primary crystallization Nylon 12 undergoes regime I kinetics. The work of chain folding, q, was calculated as 1.93 E−20 J per molecular chain fold.

The nonisothermal crystallization kinetics of Nylon 12 was studied using a number of different models. It was concluded from the Jeziorny modified Avrami treatment that a clear two stage crystallization process existed for Nylon 12. The value of n_1 was in the range 2–3, which corresponds to a two stage athermal/thermal branching fibrillar growth mechanism. The value of n_2 from the secondary stage of the crystallization ranged from 1.6 to 2.7. The reduction in the value of n_2 compared to n_1 is due to the spherulite impingement and crowding. The Ozawa equation did not model the nonisothermal crystallization kinetics of Nylon 12, in that the

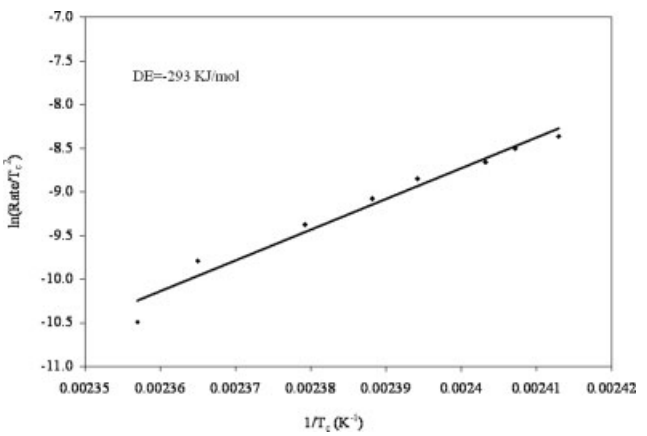

Figure 23 Plot of ln λ/T_c^2 versus $1/T_c$ (activation energy from Kissinger method for Nylon 12).

plot obtained showed a two-stage process with two values of m, where Ozawa reported for the equation to be valid only one value of m should exist. Using the Cazé model, a value of $n = 0.292$ was determined, implying this method was also ineffective in predicting a suitable value of n for Nylon 12. The Cazé method did not take into account the effect of secondary crystallization, thus assuming a much slower primary crystallization region and a low value of n. The method described by Chuah was then used to predict an average value of n for the primary stage of crystallization and good agreement between this model and the experimental data for Nylon 12 produced an average value of $n = 4.56$. This method does not fully describe the interpretation of the exponent n and complementary information on the morphology and crystallization mechanism is required.

A combined Avrami/Ozawa treatment successfully models the two-stage nonisothermal crystallization process of Nylon 12. Good agreement was recorded for specific values of $X(t)$ in a plot of log time versus log cooling rate. The values of both b and $F(T)$ were found to be strongly rate dependent in the case of Nylon 12 and can be fitted to linear functions of the form $b = AX(t) + C$ and $\log F(T) = DX(t) + E$. The activation energy for the nonisothermal crystallization processes of Nylon 12 determined using the Kissinger method was −293 kJ/mol, similar to that calculated previously for Nylon 6,6 (−331 kJ/mol)[33] and Nylon 11 (−328kJ/mol).[45]

The authors thank Degussa and Mr Thomas Groβe-Puppendahl for providing the Nylon 12 and for helpful discussions. They also acknowledge the technical assistance of Miss Paula Douglas and Dr Bronagh Millar.

NOMENCLATURE

T_m = Melting temperature
T_c = Crystallization temperature
T = Time
$X(t)$ = Relative crystallinity to time t
k_1 = Isothermal crystallization rate constant
n = Avrami exponent
$t_{[1/2]}$ = Half-time of crystallization
K = Rate parameter
$\tau_{[1/2]}$ = Rate of crystallization (reciprocal of $t_{[1/2]}$)
t_{max} = Maximum crystallization rate
ΔE = Activation energy
G = Spherulitic growth rate
G_0 = Pre-exponential factor
k = Boltzmann constant
ΔE^* = Free energy of activation for transporting a chain segment from the supercooled to the crystalline phase
ΔF^* = Free energy of formation of a crystalline nucleus of critical size
χ = Parameter related to heat of fusion and interfacial free energy
T^0_m = Equilibrium melting temperature
ΔT = Degree of supercooling
U^* = Activation energy for the transport of a macromolecule in the melt
R = Universal gas constant
T_∞ = Temperature below which all motion associated with viscous flow stop
f = Correction term (negligible at high temperature)
K_g = Energy required for the formation of a nucleus of critical size
σ = Apparent lateral free energy
σ_e = End surface free energy
b_o = Thickness of a macromolecular layer in a crystal
ΔH^0_f = Bulk enthalpy of fusion per unit volume
a_o = Width of a molecular chain in the crystal
q = Work of chain folding
A_o = Cross-sectional area of a chain in a crystal
α = Empirical constant
$\sigma_e{}^o$ = Value of σ_e, assuming no work required to form a fold
T_{disp} = Display temperature
λ = Cooling/heating rate
T_{con} = Crystallization onset temperature
T_{coff} = Crystallization offset temperature
$X(T)$ = Relative crystallinity
Z_c,Z_t = Rate parameter
m = Ozawa exponent
X_v = Volume fraction
ρ_a = Density of amorphous phase
ρ_c = Density of crystal phase
α_a = Thermal expansion coefficient of amorphous phase
α_c = Thermal expansion coefficient of crystalline phase
T_g = Glass transition temperature

References

1. Wunderlich, B. Macromolecular Physics, Vol. 3; New York: Academic Press, 1976.
2. Evans, U. R. Trans Faraday Soc 1945, 41, 365.
3. Poisson, S. D. Recherche sur la Probabilité des Jugements en matière criminelle et en matière civile, Paris: Bachelier, 1837.
4. Mears, P. Polymers: Structures and Properties; Van Nostrand: New York, 1965.
5. Hay, J. N. Br Polym J 1971, 3, 74.
6. Di Lorenzo, M. L. Prog Polym Sci 2003, 28, 663.
7. Wunderlich, B. Thermochima Acta 2003, 396, 33.
8. Long, Y.; Shanks, R. A.; Stachurski, Z. H. Prog Polym Sci 1995, 20, 651.
9. Di Lorenzo, M. L.; Silvestre, C. Prog Polym Sci 1999, 24, 917.
10. Martins, J. A.; Cruz Pinto, J. J. C. Polymer 2000, 41, 6875.

11. Hammami, A.; Spruiell, J. E.; Mehrotra, A. K. Poly Eng Sci 1995, 35, 797.
12. Mubarak, Y.; Harkin-Jones, E. M. A.; Martin, P. J.; Ahmad, M. Polymer 2001, 42, 3171.
13. Wasiak, A. Polymer 2001, 42, 9025.
14. Tjong, S. C.; Xu, S. A. Polym Int 1997, 44, 95.
15. Li, J.; Zhou, C.; Gang, W. Polym Test 2003, 22, 217.
16. Razavi-Nouri, M.; Hay, J. N. Polym Int 2006, 55, 6.
17. Silvestre, C.; Cimmino, S.; D'Alma, E.; Di Lorenzo, M. L.; Di Pace, E. Polymer 1999, 40, 5119.
18. Blom, H. P.; Teh, J. W.; Bremner, T.; Rudin, A. Polymer 1998, 39, 4011.
19. Sajkiewicz, P.; Carpaento, L.; Wasiak, A. Polymer 2001, 42, 5365.
20. Colomer Vilanova, P.; Montserrat Ribas S.; Guzman, G. M. Polymer 1985, 26, 423.
21. Lee, S. W.; Ree, M.; Park, S. E.; Jung, Y. K.; Park, C.-S.; Jin, Y. S.; Bae, D. C. Polymer 1999, 40, 7137.
22. Lee, J. W.; Lee, S. W.; Lee, B.; Ree, M. Macromol Chem Phys 2001, 202, 3072.
23. Zhang, Y.; Gu, L. Eur Polym J 2000, 36, 759.
24. Minkova, L. I.; Magagnini, P. L. Polymer 1995, 36, 2059.
25. López, L. C.; Wilkes, G. L. Polymer 1989, 30, 882.
26. Srinivas, S.; Babu, J. R.; Riffle, J. S.; Wilkes, G. L. Polym Eng Sci 1997, 37, 497.
27. Jenkins, M. J. Polymer 2001, 42, 1981.
28. Liu, T.; Mo, Z.; Zhang, H. J Polym Eng 1998, 18, 283.
29. Zhang, X.; Liu, Y.; Gao, J.; Huang, F.; Song, Z.; Wei, G.; Qiao, J. Polymer 2004, 45, 6959.
30. Kim, J. J.; Seo, S. W. Textile Res J 1994, 64, 427.
31. Liu, X.; Wu, Q. Eur Polym J 2002, 38, 1383.
32. Albano, C.; Sciamanna, R.; Gónzalez, R.; Papa, J.; Navarro, O. Eur Polym J 2001, 37, 851.
33. Zhang, Q.; Mo, Z. Chin J Polym Sci 2001, 19, 237.
34. Liu, S.; Yu, Y.; Cui, Y.; Zhang, H.; Mo, Z. J Appl Polym Sci 1998, 70, 2371.
35. Liu, M.; Zhao, Q.; Wang, Y.; Zhang, C.; Mo, Z.; Cao, S. Polymer 2003, 44, 2537.
36. Ren, M.; Mo, Z.; Chen, Q.; Song, J.; Wang, S.; Zhang, H.; Zhao, Q. Polymer 2004, 45, 3511.
37. Avrami, M. J Chem Phys 1939, 7, 1103.
38. Avrami, M. J Chem Phys 1940, 8, 212.
39. Avrami, M. J Chem Phys 1941, 9, 177.
40. Cojazzi, C. J Polym Sci Part A: Polym Chem 1972, 10, 289.
41. Arimoto, H.; Ishibashi, M.; Hiral, M.; Chatani, Y. J Polym Sci Part A: Polym Chem 1965, 3, 317.
42. Cojazzi, C. Makromol Chem 1973, 168, 289.
43. Cebe, P.; Hong, S. D. Polymer 1986, 27, 1183.
44. Turnbull, D.; Fisher, J. C. J Chem Phys 1949, 17, 71.
45. Ziabicki, A. Coll Polym Sci 1974, 252, 433.
46. Hoffman, J. D.; Davis, G. T.; Lauritzen, J. I. Treatise on Solid State Chemistry, Vol. 3; Plenum Press: New York, 1976.
47. Hoffman, J. D. Polymer 1983, 24, 3.
48. Hoffmann, J. D.; Miller, R. L. Polymer 1997, 38, 3151.
49. Aharoni, S. M. *n*-Nylons: Their Synthesis, Structure and Properties; Wiley: Chichester, 1997.
50. Lim, G. B. A.; Lloyd, D. R. Polym Eng Sci 1993, 33, 537.
51. Gogolewski, S.; Czerniawska, K.; Gasiorek, M. Coll Polym Sci 1980, 258, 1130.
52. Chuah, K. P.; Gan, S. N.; Chee, K. K. Polymer 1999, 40, 253.
53. Lauritzen, J. I.; Hoffman, J. D. J Appl Phys 1973, 44, 4340.
54. Lauritzen, J. I.; Hoffman, J. D. J Res Natl Bur Stand (US) 1960, 64A, 73.
55. Monasse, B.; Haudin, J. M. Coll Polym Sci 1985, 265, 822.
56. Jeziorny, A. Polymer 1978, 19, 1142.
57. Mandlekern, L. Crystallization of Polymers; McGraw-Hill: New York, 1964.
58. Liu, Z.; Maréchal, P.; Jérôme, R. Polymer 1997, 38, 5149.
59. Ozawa, T. Polymer 1971, 12, 150.
60. Cazé, C.; Devaux, E.; Crespy, A.; Cavrot, J. P. Polymer 1997, 38, 497.
61. Van Krevelen, D. W.; Hoftyzer, P. J.; Properties of Polymers; Elsevier Scientific Publishing: Amsterdam, 1976.
62. Pfliiger, R. Polymer Handbook, Vol. 109; Wiley-Interscience: New York, 1989.
63. Maneschalchi, F.; Rossi, R.; Mattiussi, A. Eur Polym J 1973, 9, 601.
64. Mo, Z. Polym Eng Sci 1997, 27, 568.
65. Kissinger, H. E. J Res Natl Bur Stand (US) 1956, 57, 217.